JOURNAL OF APPLIED ELECTROCHEMISTRY **15** (1985) 837–858

Reactor engineering models of complex electrochemical reaction schemes. III. Galvanostatic operation of parallel reactions in batch reactors

KEITH SCOTT

Department of Chemical Engineering, Teesside Polytechnic, Middlesbrough, Cleveland, TS1 3BA, UK

Received 13 June 1984; revised 27 March 1985

Batch electrochemical reactor models for parallel reaction sequences are developed for cells operating galvanostatically. Independent and dependent parallel reactions and a parallel–series reaction scheme are considered and emphasis is placed on the development of analytical expressions to predict reactor behaviour. Electro-organic synthesis reactions such as the production of beta-alanine and glyoxylic acid are considered as examples. Experimental data for the electro-oxidation of aqueous oxalic acid and glyoxylic acid solutions are shown to be in reasonable agreement with the reaction analysis.

Nomenclature

a	Parameter defined in Equation 21
C_j^s	Surface concentration of species j
C_j	Bulk concentration of species j
C_{jo}	Initial concentration of species j
C_{Bmax}	Maximum concentration of species B
CE	Current efficiency
E	Electrode potential
F	Faraday constant
i_p	Partial current density of step p of reaction scheme
i_T	Total current density
k_{fp}	Forward electrochemical rate constant of step p
k_{Lj}	Mass transfer coefficient for species j
K_L	Dimensionless mass transfer parameter
n_p	Number of electrons in step p of reaction scheme
S	Electrode area
t	Reaction time
V	Batch reactor volume
β_p	Constant describing potential dependency of reaction rate constant of reaction step p
Y_1, Y_2, Y_3	Effective overall resistance factors
τ_g	Dimensionless reaction time for galvanostatic operation
τ_p	Dimensionless reaction time for potentiostatic operation

1. Introduction

In recent years significant advances in electrochemical reactor design and analysis have been made by the application and development of well-known concepts in chemical engineering. Reactor designs such as fluidized beds, trickle tower cells, shear flow cells, two phase contactors, etc., are just

0021–891X/85 $03.00 + .12

a few examples of this approach as well as the subsequent analysis of contacting patterns using tracer techniques [1].

The analysis of 'complex' electrochemical reaction sequences in reactors of known contact patterns, i.e. mass transport and fluid mechanics, may also be based on accepted chemical reaction engineering techniques [2]. Many studies of multiple electrochemical reactions using porous or particulate bed electrodes have appeared in the literature and are reviewed in [3]. Theoretical considerations of series reactions and parallel reactions in flow reactors with electrodes of approximate flat plate configuration have been made by Sakellaropoulos [4, 5]. The effect of interphase mass transport was not considered in this work but was included in a later analysis of parallel reactions in continuous stirred tank reactors [6]. Previous analyses related to this work have looked at series and parallel reactions when mass tranport has a controlling influence on operation [7] and included a chemical reaction step [8]. The effect of operating parameters, such as electrode potential and mass transport, on reactor selectivity and current efficiency was investigated. The adoption of potentiostatic control, however, limits the applicability of the analyses. This paper continues the analysis of complex reaction sequences, looking specifically at parallel reactions during galvanostatic operation. This type of operation is more important industrially because of its relative cost effectiveness and ease of control and operation in comparison to potentiostatic operation. To illustrate the presented models a number of potentially important industrial electro-organic syntheses are analysed. These are the reduction of cyanoacetic acid to beta-alanine and the reduction of oxalic acid to glyoxylic acid. One of these is used as an example of the analysis of a parallel–series reaction network.

A number of simplifying assumptions are made in this analysis regarding kinetics, mechanisms and transport properties. These include the representation of mass transport by one parameter, i.e. a mass transport coefficient, the use of Tafel kinetics and pseudo first order reactions, and the disregard of the reaction mechanism being a set of elementary steps. However, using experimental data for the electro-oxidation of aqueous oxalic acid and glyoxylic acid solutions, the applicability of the analysis is shown.

2. Experimental details

2.1. *The electro-oxidation of oxalic acid and glyoxylic acid*

The experimental procedures for the electro- oxidation of aqueous solutions of oxalic acid and glyoxylic acid are described in this section. This work was undertaken to investigate the purification (i.e. removal of oxalic acid) of an aqueous solution of glyoxylic acid.

Electrolyses were performed in a divided plate and frame flow cell, operating in a batch recirculation mode. The anode was graphite of area 200 cm^2 and the cathode was lead of area 200 cm^2. The anolyte (4 litres) consisted of either aqueous solutions of oxalic acid, varying from approximately 0.1 to 1.0 M, an aqueous solution of glyoxylic acid, 0.22 M, or an aqueous solution of both acids. Anolyte solutions were separated from an aqueous sulphuric acid catholyte by an Ionac cation-exchange membrane. Flow characteristics in the cell were turbulent with Reynolds numbers of approximately 10 000.

Batch electrolyses were carried out at constant current densities and at a constant temperature of 20° C, maintained by a mains water heat exchanger situated in the flow circuit. Polarization data were obtained in a similar flow cell in which the electrode area was 10 cm^2.

The analyses of oxalic acid and glyoxylic acid were both carried out volumetrically; oxalic acid by titration with potassium permanganate solution, and glyoxylic acid by the back titration (using iodine) of the sodium bisulphite solution remaining after the reaction of glyoxylic acid with sodium bisulphite to form the bisulphite compound.

2.2. *The electroreduction of oxalic acid*

Electrolysis was performed in the same divided plate and frame flow cell and flow circuit as for the electro-oxidation of oxalic acid. The cathode was lead of purity 99.99% and the anode either lead, thallium alloy or dimensionally stable anode (ruthenium dioxide based composite on titanium) supplied by Oronzio de Nora, Milano, Italy. The catholyte consisted of a saturated aqueous solution of oxalic acid separated from an aqueous sulphuric acid anolyte by an Ionac cation exchange membrane. Batch electrolyses were carried out at constant current densities at temperatures in the range 8–22° C. Flow characteristics were again turbulent.

3. Reactor analysis and results

The mathematical analysis considers parallel reaction schemes operating in electrochemical reactors in a batch mode. The kinetics of the reaction steps are assumed to be of the Tafel type, i.e. irreversible, and the reaction rates are influenced by mass transport, which is defined by way of a mass transfer coefficient k_{Lj} for each species j. Reactor operation is in the galvanostatic mode and all reactions are assumed first order.

Three reaction schemes are considered overall:

(a) Two independent parallel reactions (one reaction being gas evolution).
(b) Two dependent parallel reactions.
(c) A parallel–series reaction scheme.

The latter is considered to be representative of the electroreduction of oxalic acid to glyoxylic acid (the product), which can be further reduced to glycolic acid and glyoxal according to a parallel mechanism. The electroreduction of oxalic acid in acidified aqueous media can be written as

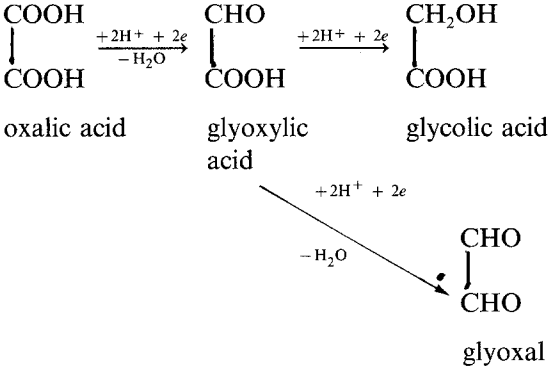

The following analysis concentrates on limiting situations, with the main assumption that the Tafel slopes for competing reactions are integer ratios. This assumption should not significantly detract from the use of the equations since a wide variety of reaction schemes fit this situation.

3.1. *Two independent reactions*

The reaction scheme is of the form

$$A + n_1 e \xrightarrow{k_{f1}} B$$

$$C + n_2 e \xrightarrow{k_{f2}} D$$

Following a previous analysis [7], the reaction rates can be expressed as

$$\frac{i_1}{n_1 F} = \frac{C_A}{Y_1} \tag{1}$$

$$\frac{i_2}{n_2 F} = \frac{C_C}{Y_2} \tag{2}$$

with

$$Y_1 = \frac{1}{k_{f1}} + \frac{1}{k_{LA}}$$

$$Y_2 = \frac{1}{k_{f2}} + \frac{1}{k_{LC}}$$

where C_A and C_C are bulk concentrations, k_{f1}, k_{f2} are forward electrochemical rate constants and k_{LA} and k_{LC} are mass transfer coefficients. k_{f1} and k_{f2} are of the form

$$k_{f1} = k_1 \exp(\beta_1 E)$$

where E is the electrode potential.

Under galvanostatic conditions the total currenty density i_T is constant and is given by

$$i_T = i_1 + i_2 \tag{3}$$

For a batch reactor of electrode area S and volume V, material balances for A and C are

$$-\frac{dC_A}{dt} = \frac{S}{V}\left(\frac{i_1}{n_1 F}\right) \tag{4}$$

$$-\frac{dC_C}{dt} = \frac{S}{V}\left(\frac{i_2}{n_2 F}\right) \tag{5}$$

Combining Equations 3, 4 and 5 we obtain

$$\frac{dC_C}{dt} + \frac{n_1}{n_2}\left(\frac{dC_A}{dt}\right) = -\frac{S}{V}\left(\frac{i_T}{n_2 F}\right) \tag{6}$$

with the conditions that

$$t = 0, \qquad C_A = C_{Ao}, \qquad C_C = C_{Co}$$

The solution is

$$C_C - C_{Co} + \frac{n_1}{n_2}(C_A - C_{Ao}) = -\frac{S}{V}\left(\frac{i_T}{n_2 F}\right)t \tag{7}$$

Dividing Equation 4 by Equation 5 and substituting (1) and (2) gives

$$\frac{dC_A}{dC_C} = \left(\frac{C_A}{C_C}\right)\left(\frac{Y_2}{Y_1}\right) \tag{8}$$

This can be solved for certain simplified situations. If both reactions are at their limiting currents then

$$\frac{Y_1}{Y_2} = \frac{k_{LB}}{k_{LA}} = 1$$

or if both reactions are kinetically slow, such that mass transport does not influence performance, then for $\beta_1 = \beta_2$

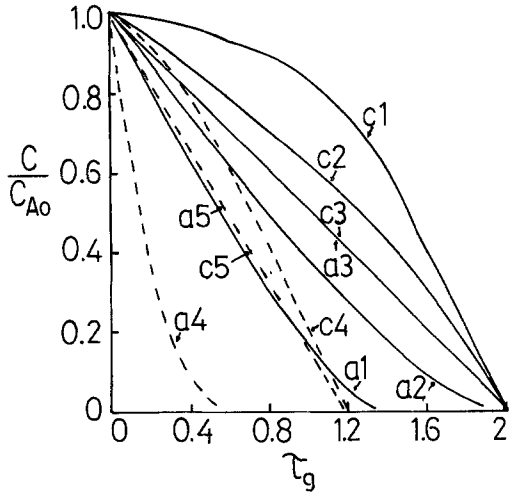

Fig. 1. Concentration time characteristics for two independent Tafel reactions.

$$\tau_g = \frac{Si_T t}{VnFC_{Co}}; \; n_1 = n_2$$

(——) $C_{Co} = C_{Ao}$.

(– – –) $C_{Co} = 10\,C_{Ao}$.

C_{Co}/C_{Ao}	1	1	1	10	10
k_1/k_2	10	2	1	10	1
C_C/C_{Ao}	c1	c2	c2	c4	c5
C_A/C_{Ao}	a1	a2	a3	a4	a5

$$\frac{dC_A}{dC_C} = \left(\frac{k_1}{k_2}\right)\left(\frac{C_A}{C_C}\right) \tag{9}$$

giving

$$\frac{C_A}{C_{Ao}} = \left(\frac{C_C}{C_{Co}}\right)^{k_1/k_2} \tag{10}$$

which, coupled with Equation 7, gives

$$\frac{C_C - C_{Co}}{C_{Ao}} + \frac{n_1}{n_2}\left[\left(\frac{C_C}{C_{Co}}\right)^{k_1/k_2} - 1\right] = -\frac{S}{V}\left(\frac{i_T}{n_2 F C_{Ao}}\right)t \tag{11}$$

From Equations 11, 7 and 10 fractional conversions of A and C, as a function of time, can be obtained. Typical concentration, time characteristics for this system are presented in Fig. 1. The time scale is in fact the Faradays per mole of C passed, i.e. $\tau_g = si_T t/Vn_2FC_{Co}$. Two main factors influence the decay of concentration of A and C with time: the ratio of the rate parameters k_1/k_2 and the initial concentrations of both species. With equal initial concentrations of both components, the step with the greater rate constant exhibits the more rapid decrease in concentration. When $k_1 \gg k_2$ the conversion of C is only significant when C_A is low. The concentration C_C then follows the expected linear decrease in concentration, characteristic of a single Tafel reaction.

When the initial concentrations of the two components are widely different, e.g. $C_{Co} = 10\,C_{Ao}$, the conversion of C, as expected, increases for similar ratios of k_1/k_2.

If the two reactions had unequal Tafel slopes, the conversion of the component with the higher Tafel slope would become more favourable with time, due to the increase in electrode potential caused by galvanostatic operation.

3.1.1. Gas evolution as the second reaction. A common situation in electrochemical systems is for the secondary reaction to be gas evolution, e.g. hydrogen, which can typically occur without mass transport limitations so that the reaction rate can be written as

$$\frac{i_3}{n_3 F} = k_{f3} = k_3 \exp(\beta_3 E) \tag{12}$$

The total current in this system is given by

$$i_T = \frac{n_1 F C_A}{Y_1} + n_3 F k_{f3} \tag{13}$$

By combining Equation 13 with Equations 1 and 4 the potential variation can be obtained (see Appendix A) as

$$\frac{1}{k_{f1o}} - \frac{1}{k_{f1}} + \frac{1}{k_{LA}} \ln\left(\frac{i_T - n_3 F k_{f3o}}{i_T - n_3 F k_{f3}}\right) + \int_{E_o}^{E} \frac{n_3 F \beta_3 (k_{f3}/k_{f1})}{(i_T - n_3 F k_{f3})} dE = \left(\frac{S}{V}\right) t \tag{14}$$

where the subscript o denotes initial values of parameters.

A final integration of Equation 14 to give analytical expressions for the potential variation as a function of time can be achieved for a number of integer ratios of β_3 to β_1. With the condition $\beta_3 = \beta_1$ Equation 14 becomes

$$\frac{1}{k_{f1o}} - \frac{1}{k_{f1}} + \frac{1}{k_{LA}} \ln\left(\frac{i_T - n_3 F k_{f3o}}{i_T - n_3 F k_{f3}}\right) + \frac{n_3 F (k_3/k_1)}{i_T} \ln\left[\left(\frac{k_{f3}}{k_{f3o}}\right)\left(\frac{i_T - n_3 F k_{f3o}}{i_T - n_3 F k_{f3}}\right)\right] = \left(\frac{S}{V}\right) t \tag{15}$$

This equation defines the potential variation with time during electrolysis.

Substituting Equations 1, 3 and 12 into 15 gives the following expression for the concentration of A as a function of E and t.

$$-\left[\frac{1}{k_{LA}} + \frac{n_3 F (k_3/k_1)}{i_T}\right] \ln\left(\frac{C_{Ao}}{C_A}\right) = \frac{1}{k_{f1o}} - \frac{1}{k_{f1}} + \left[\frac{1}{k_{LA}} + \frac{n_3 F (k_3/k_1)}{i_T}\right] \ln\left(\frac{Y_1}{Y_{1o}}\right) + \frac{nF(k_3/k_1)}{i_T} \ln\left(\frac{k_{f3}}{k_{f3o}}\right) - \left(\frac{S}{V}\right) t \tag{16}$$

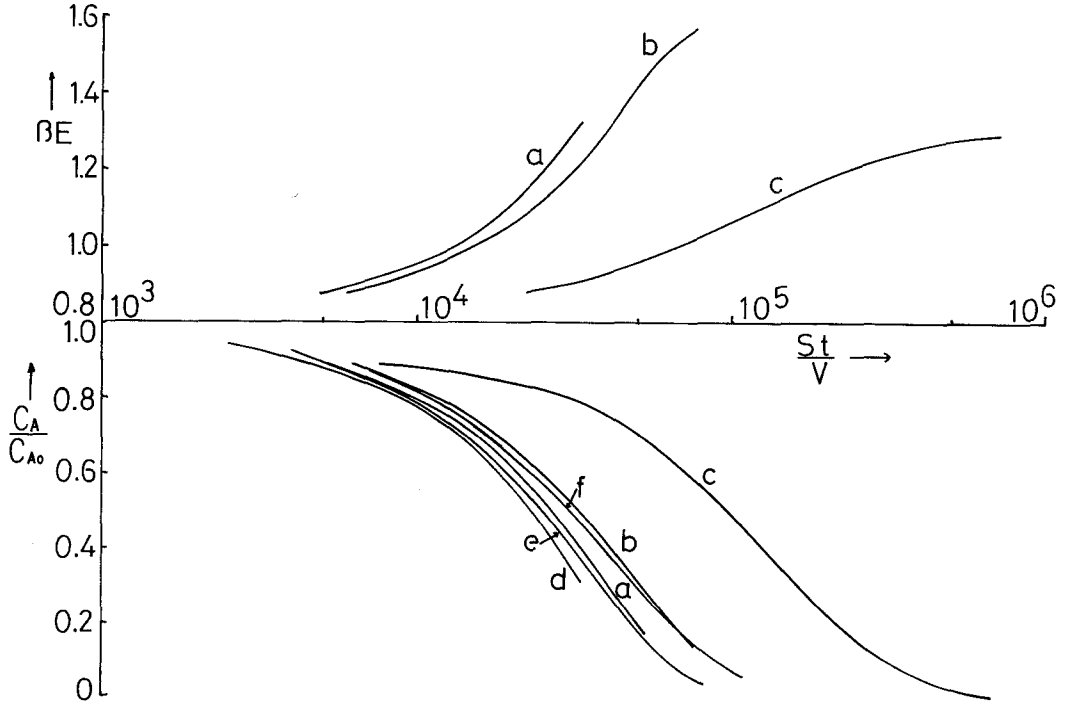

Fig. 2. Variation of concentration and electrode potential for a Tafel reaction accompanied by solvent decomposition. $\beta_1 = \beta_3$; $n_1 = n_3$; $C_{Ao} = 100\,\text{mol m}^{-3}$; $k_3 = 5 \times 10^{-4}\,\text{mol m}^{-2}\,\text{s}^{-1}$. k_1/k_3: (a–c) 0.02; (d–f) 0.04. k_{LA}(m s^{-1}): (a) 10^{-3}; (b) 10^{-4}; (c) 10^{-5}; (d) 10^{-3}; (e) 10^{-4}; (f) 4×10^{-5}. βE_o: (a–c) 0.8; (d) 0.201; (e) 0.382; (f) 0.693. i_T/nF ($\times 10^3$): (a) 3.294; (b) 3.29; (c) 1.8; (d–f) 3.

Hence Equations 15 and 16 can be combined to determine the variation of concentration of A with time. Typical variations in the concentration of A and in the electrode potential are given in Fig. 2. At a fixed initial electrode potential [E_o], the influence of a decrease in mass transport rate is to slow down the rate of conversion of A, due to the lower applied total current. The rate of increase of electrode potential is also reduced at lower mass transport rates.

At a fixed total current density, the effect of a decrease in mass transport rate is again to reduce the rate of conversion of A. Current efficiencies for the conversion of A are reduced significantly by low rates of mass transport (see Fig. 3) and under the conditions considered can be more than halved. The expected effect of an increase in the ratio of the kinetic rate constants k_1/k_3, that is, an increase in current efficiency, is shown in Fig. 3. Increasing the current density is also shown in Fig. 3 to decrease current efficiency for fixed values of kinetic and mass transport parameters.

Under kinetic control the resultant expression for the concentration of A can be written as

$$(C_A - C_{Ao}) + \left(\frac{n_3}{n_1}\right)\left(\frac{k_3}{k_1}\right) \ln\left(\frac{C_A}{C_{Ao}}\right) = -\frac{Si_T t}{Vn_1 F} \tag{17}$$

In the absence of the secondary hydrogen evolution ($k_3 = 0$), Equation 17 gives the expected linear decrease of concentration with time during galvanostatic operation.

The variation of the concentration of A with the Faradays per mole of A passed is shown in Fig. 4a as a function of the parameter $n_3k_3/n_1k_1C_{Ao}$. As expected, the higher the value of this parameter the slower the decrease in the concentration of A. The overall current efficiencies for the reaction, which are shown in Fig. 4b as a function of reactant concentration, reflect the poor conversions obtained at high values of $n_3k_3/\ n_1k_1C_{Ao}$.

Another simple limiting case of this analysis is when the main reaction is operating at the limiting current throughout the electrolysis period. As a consequence of reactant depletion, the rate of hydrogen evolution increases with time due to the inevitable increase in electrode potential.

The variation of reactant concentration with time is given by

$$\frac{C_A}{C_{Ao}} = \exp\left(-\frac{Sk_{LA}t}{V}\right) \tag{18}$$

the classic exponential decrease. The variation of electrode potential is given by

$$n_3Fk_3 \exp(\beta_3 E) = i_T - n_1Fk_{LA}C_{Ao} \exp(-k_{LA}St/V) \tag{19}$$

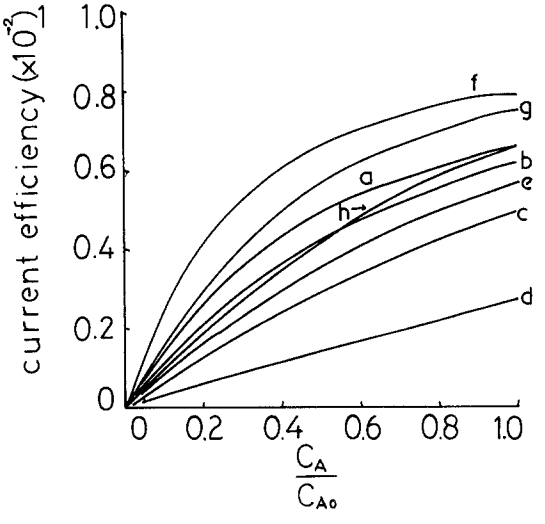

Fig. 3. Variation of differential current efficiency with reactant concentration for a reaction obeying Tafel kinetics accompanied by solvent decomposition. $\beta_1 = \beta_3$; $n_1 = n_3$; $C_{Ao} = 100\,mol\,m^{-3}$; $k_3 = 5 \times 10^{-4}\,mol\,m^{-2}\,s^{-1}$. k_1/k_3: (a–e) 0.02; (f–h) 0.04. k_{LA} ($m\,s^{-1}$): (a) 10^{-3}; (b) 10^{-4} (c) 3×10^{-5} (d) 10^{-5}; (e) 10^{-4}; (f) 10^{-3}; (g) 10^{-4}; (h) 4×10^{-5}. i_T/nF ($\times 10^3$): (a–d) 3; (e) 6; (f–h) 3.

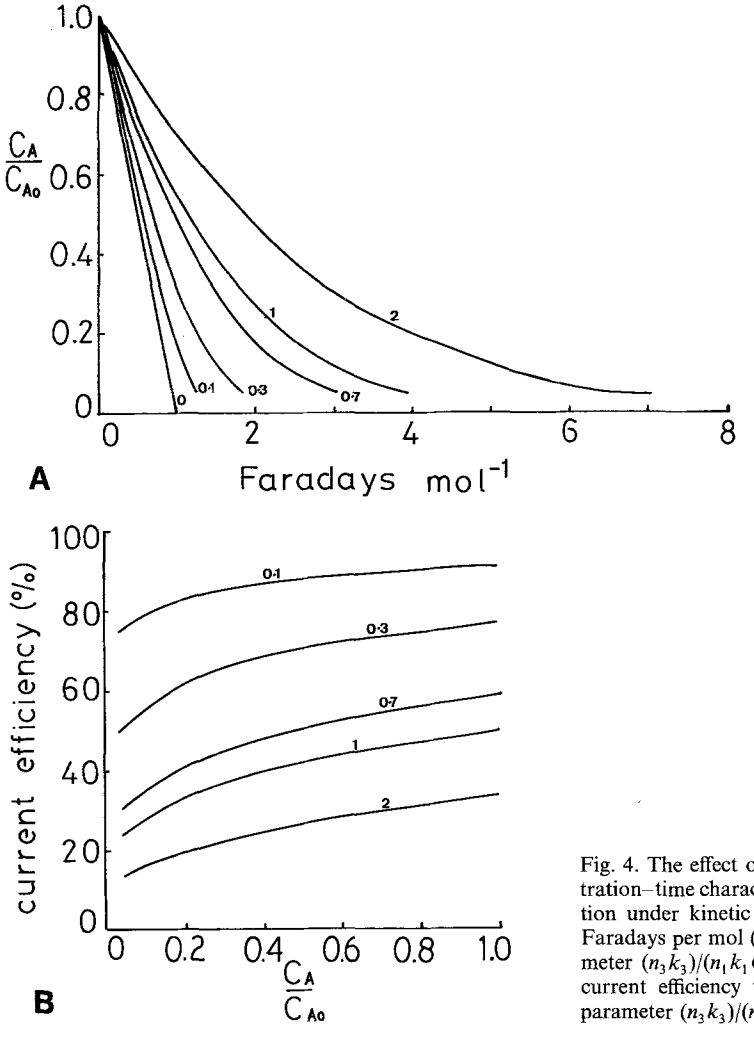

Fig. 4. The effect of solvent decomposition on the concentration–time characteristics and current efficiency for a reaction under kinetic control. (A) Variation of C_A/C_{Ao} with Faradays per mol $(Si_T t)/(Vn_1 FC_{Co})$ passed. Values of parameter $(n_3k_3)/(n_1k_1C_{Ao})$ on figure. (B) Variation of overall current efficiency with reactant concentration. Values of parameter $(n_3k_3)/(n_1k_1C_{Ao})$ on figure.

and the overall current efficiency for the reaction is

$$\frac{n_1 FVC_{Ao}\left[1 - \exp\left(-\frac{k_{LA}St}{V}\right)\right]}{Si_T t} \tag{20}$$

Current efficiencies predicted from this expression are presented in Fig. 5 for various values of a mass transfer parameter $K_L = k_{LA}n_1FC_{Ao}/i_T$. This parameter is the ratio of the maximum limiting current to the total current; and as such, the lower its value the lower the current efficiency for the same charge passed. The anticipated fall in current efficiency with charge passed is also seen in Fig. 5.

3.1.2. Electro-organic process example. To illustrate the use of the above model equations, consider the reduction of cyanoacetic acid to beta-alanine hydrochloride in aqueous HCl using a deposited palladium black over graphite cathode. The published work of Krishnan *et al.* [9] is relevant to the

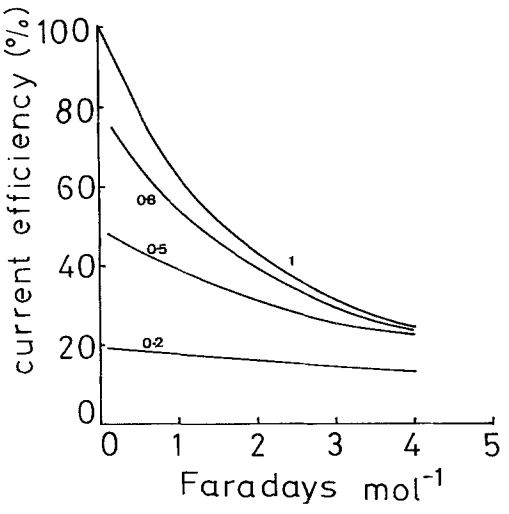

Fig. 5. Current efficiencies for a Tafel reaction operating at its limiting current. Values of mass transfer parameter $K_L = (k_{LA} n_1 F C_{Ao})/i_T$ given on figure.

example. The reaction is

$$NCCH_2COOH \xrightarrow[+\ HCl]{4H^+ + 4e} HClH_2NCH_2CH_2COOH$$

and occurs simultaneously with the hydrogen reduction reaction.

The polarization characteristics of both reactions from [9] are reasonably well represented by the following expressions.

$$i_1 = 12.8 \exp\left(\frac{2.3E}{130}\right) \qquad A\ m^{-2}$$

and for hydrogen reduction

$$i_3 = 0.14 \exp\left(\frac{2.3E}{65}\right) \qquad A\ m^{-2}$$

With $\beta_1 = \beta_3/2$ Equation 14 can be integrated to give

$$\frac{St}{VC_{Ao}} = \frac{1}{C_{Ao}k_{f1o}} - \frac{1}{C_{Ao}k_{f1}} + \frac{1}{C_{Ao}k_{LA}} \ln\left(\frac{i_T - n_3 F k_{f3o}}{i_T - n_3 F k_{f3}}\right) + \frac{1}{k_1 C_{Ao}(a)^{1/2}} \ln\left(\frac{(a)^{1/2} + \exp(\beta_1 E)}{(a)^{1/2} - \exp(\beta_1 E)}\right) \tag{21}$$

where $a = i_T/n_3 F k_3$.

The predicted conversion of cyanoacetic acid as a function of time is presented in Fig. 6 for current densities varying from 100 to 1500 A m^{-2} using the values

$$S/VC_{Ao} = 0.213, \text{ and } C_{Ao}k_{LA} = 2 \times 10^{-3}.$$

The behaviour shows the expected trend in this type of reaction sequence; that is, a gradual decay in the rate of production (and current efficiency) as the secondary hydrogen reduction reaction becomes more dominant and mass transport limitations become important at low reactant concentrations.

Experimental data of Krishnan *et al.* [9] are also shown on Fig. 6 in the form of the concentration attained after twice the theoretical charge for complete conversion is passed. Considering the limitations in a comparison of this nature, especially due to inaccuracies in interpreting polarization data, reasonable agreement is achieved at high current densities.

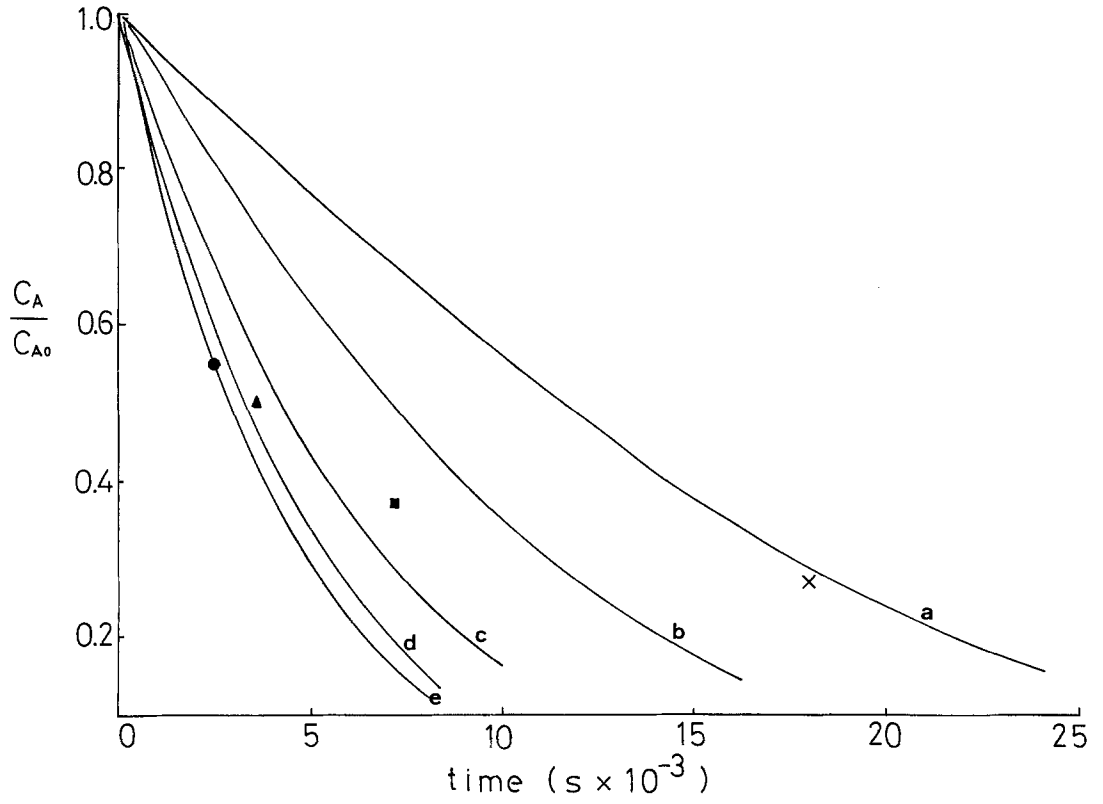

Fig. 6. Concentration variation during the reduction of cyanoacetic acid: (a) 100 A m^{-2}; (b) 200 A m^{-2} (×); (c) 500 A m^{-2} (■); (d) 1000 A m^{-2} (▲); (e) 1500 A m^{-2} (●). Experimental data of Krishnan *et al.* ●, ▲, ■, ×.

3.1.3. The electro-oxidation of oxalic acid and glyoxylic acid. In electrochemcial technology, one area which eludes the classic analysis of electrochemical kinetics is that of reactions which occur in the absence of excess supporting electrolyte. However, by combining reaction mechanisms and reactor models with limiting polarization data, such reaction systems should lend themselves to analysis sufficient to generate a reasonable model of process operation. It is in this respect that the analysis of data for the electro-oxidation of aqueous solutions of oxalic acid and glyoxylic acid [10] is now considered.

Polarization curves for the anodic oxidation of oxalic acid and glyoxylic acid are shown in Fig. 7. Tafel slopes for both acids are in the region of 180–190 mV per decade. From this data, the ratio of rate constants for oxalic acid to glyoxylic acid oxidations (k_1/k_2) is approximately 11, assuming reactions exhibit first order dependency.

Fig. 8 shows some experimental data for the oxidation of a 10 g l^{-1} solution of oxalic acid at current densities of 500 A m^{-2} and 1000 A m^{-2}. These data are plotted in accordance with Equation 17 to try and obtain the ratio of rate constants of oxalic acid oxidation and oxygen evolution (k_1/k_3) assuming equal Tafel slopes, the absence of mass transport limitations and the concentration independency of oxygen evolution. The data in Fig. 8 are correlated quite well giving a ratio of $k_1/k_3 = 32$ mol l^{-1}. Some curvature in the data is exhibited at higher conversion which is probably a result of the onset of mass transport limitations.

Experimental data for the oxidation of oxalic acid, from an aqueous solution of glyoxylic acid (80 g l^{-1}) and oxalic acid (21 g l^{-1}) at current densities of 750 A m^{-2} and 1250 A m^{-2} are given in Fig. 9. These data, in the form of oxalic acid concentration versus charge passed, are in reasonable agreement with theoretical predictions, using the above determined ratios of rate constants in the

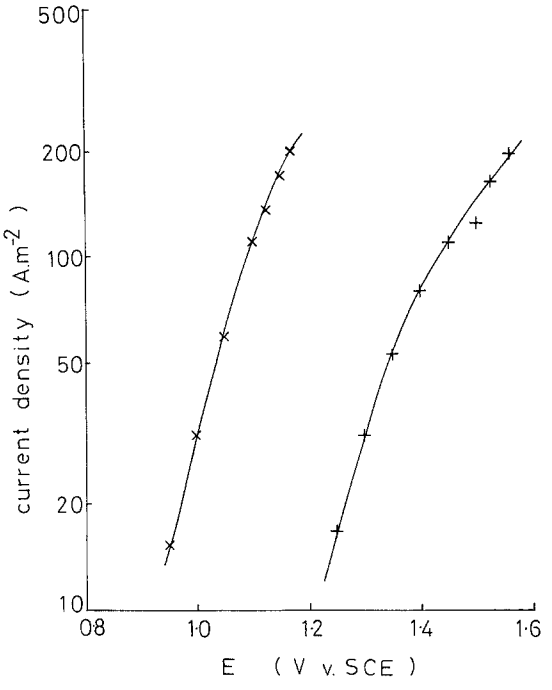

Fig. 7. Polarization curves for the electro-oxidation of oxalic acid and glyoxylic acid solutions. Temperature 20° C; Reynolds Number = 6000. ×, aqueous oxalic acid 1.0 M; +, aqueous glyoxylic acid 0.22 M.

following model equation

$$(C_A - C_{Ao}) + \left(\frac{n_3}{n_1}\right)\left(\frac{k_3}{k_1}\right) \ln\left(\frac{C_A}{C_{Ao}}\right) + \left(\frac{n_2}{n_1}\right)\left(\frac{k_1}{k_2}\right) C_{Co}\left[\left(\frac{C_A}{C_{Ao}}\right)^{k_2/k_1} - 1\right] = -\frac{Si_T t}{Vn_1 F} \tag{22}$$

This equation assumes that the Tafel slopes of the three competing reactions are equal, and is derived in Appendix B.

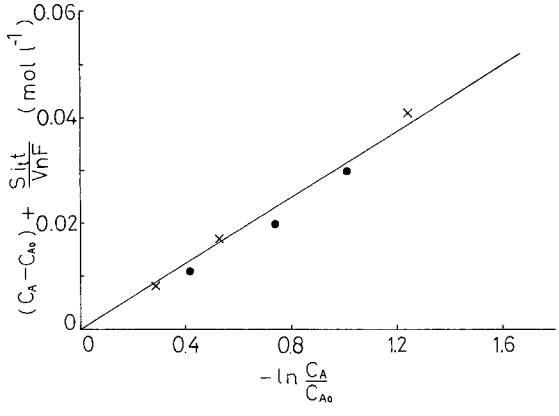

Fig. 8. Data analysis of the electro-oxidation of oxalic acid solution. Plotted in accordance with Equation 17. ×, 1000 A m^{-2}; ●, 500 A m^{-2}. Oxalic acid concentration 10 g l^{-1}, temperature 20° C.

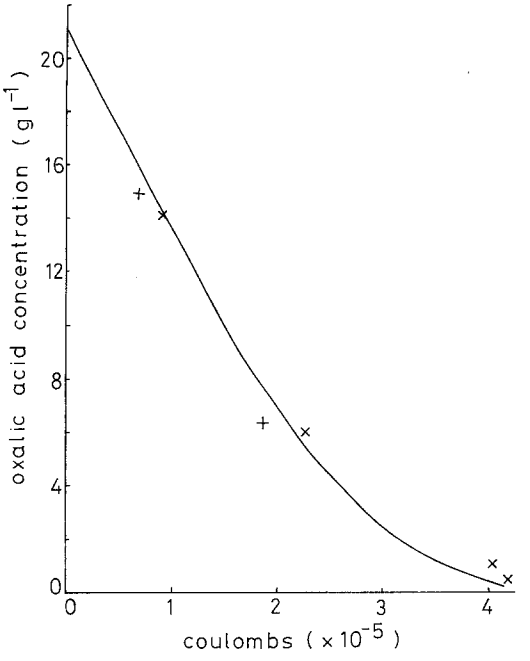

Fig. 9. Variation of oxalic acid concentration in the oxidation of an aqueous solution of oxalic acid (21 g l^{-1}) and glyoxylic acid (80 g l^{-1}). ×, 1250 A m^{-2}; +, 750 A m^{-2}; (———), theoretical prediction.

3.2. *Two dependent parallel reactions*

The reaction scheme is

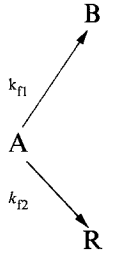

and reaction currents are given by

$$\frac{i_1}{n_1 F} = k_{f1} C_A^S \tag{23}$$

$$\frac{i_1}{n_1} = \frac{k_{f1}}{k_{f2}}\left(\frac{i_2}{n_2}\right) \tag{24}$$

$$\frac{i_1}{n_1 F} + \frac{i_2}{n_2 F} = k_L(C_A - C_A^S) \tag{25}$$

Combining these expressions with the batch reactor design equation,

$$\frac{dC_A}{dt} = -\frac{S}{V}\left(\frac{i_1}{n_1 F} + \frac{i_2}{n_2 F}\right) \tag{26}$$

the variation of electrode potential with time is obtained (see Appendix C) as

$$\frac{k_{f2}}{k_{f1}}\left\{\frac{\left[\frac{(\beta_2-\beta_1)\left(1-\frac{n_2}{n_1}\right)}{k_L}\right]-\left[\frac{n_2}{n_1}\left(\frac{\beta_2}{k_{f1}}\right)-\frac{\beta_1}{k_{f2}}\right]}{\left(1+\frac{k_{f2}}{k_{f1}}\right)\left[1+\left(\frac{n_2}{n_1}\right)\left(\frac{k_{f2}}{k_{f1}}\right)\right]}\right\}\mathrm{d}E = -\left(\frac{S}{V}\right)\mathrm{d}t \tag{27}$$

which lends itself to numerical integration. Integration of this equation can be simplified by making the substitution $u = \exp(\beta_2 - \beta_1)E$. When $n_1 = n_2$ a solution may be obtained generally from integration tables in the form of an infinite series. For certain ratios of β_2/β_1, e.g. 2 or 1/2, useful analytical solutions can be obtained (see Appendix D.) However, with the condition that $\beta_1 = \beta_2$ it can be integrated analytically to give

$$\frac{1}{1+\frac{k_2}{k_1}}\left(\frac{1}{k_{f1}}-\frac{1}{k_{f1o}}\right) = -\left(\frac{S}{V}\right)t \tag{28}$$

where k_{f1o} is the value of k_{f1} at $t = 0$. Substituting for k_{f1} using Equation 25 gives the concentration variation with time as

$$C_{Ao} - C_A = \frac{\left(1+\frac{k_2}{k_1}\right)\left[\frac{S}{V}\left(\frac{i_T}{n_1F}\right)t\right]}{\left[1+\frac{n_2}{n_1}\left(\frac{k_2}{k_1}\right)\right]} \tag{29}$$

The ratio of production of B to R (the selectivity) is given by

$$\frac{C_B}{C_R} = \frac{k_1}{k_2} \tag{30}$$

With this condition of equal Tafel slopes for the competing reactions the system behaviour is similar to that of a single Tafel equation. The conversion of reactant A varies linearly with time and the electrode potential increases exponentially with time. The selectivity for this system is constant and independent of electrode potential.

When the Tafel slopes of the competing reactions are not equal, increases in electrode potential during reaction will affect reaction selectivity through its influence on the reaction rate constants k_{f1} and k_{f2}. This is seen in Fig. 10 for the conditions $\beta_2 = \beta_1/2$, where point selectivity $\mathrm{d}C_B/\mathrm{d}C_R$ is plotted as a function of fractional conversion $X_A = 1 - (C_A/C_{Ao})$ for a range of kinetic and mass transport parameters.

For fixed values of kinetic constants and mass transport coefficient it can be seen in Fig. 6 that increasing the total reaction current favours the selectivity, i.e. favours the step of greatest Tafel slope. Here selectivities can be very much greater than for reactions with equal Tafel slopes, especially at high conversions. Even when the value of $k_2 > k_1$, reaction selectivity can still favour reaction to B.

Unlike the case of equal Tafel slopes, mass transport exhibits an influence on reaction selectivity. For systems of unequal Tafel slope the higher the value of mass transfer coefficient (seen in Fig. 10 as a decrease in k_1/k_L at fixed k_2/k_1 and $i_T/nFC_{Ao}k_1$ the lower the selectivity of the step of greatest Tafel slope. In this instance the quest for high rates of mass transport, often sought in electrosynthesis, is not desirable on the grounds of selectivity. However, because the rate of reactant conversion is slow at low mass transport rates, a compromise between high selectivity and high reaction rate may be necessary.

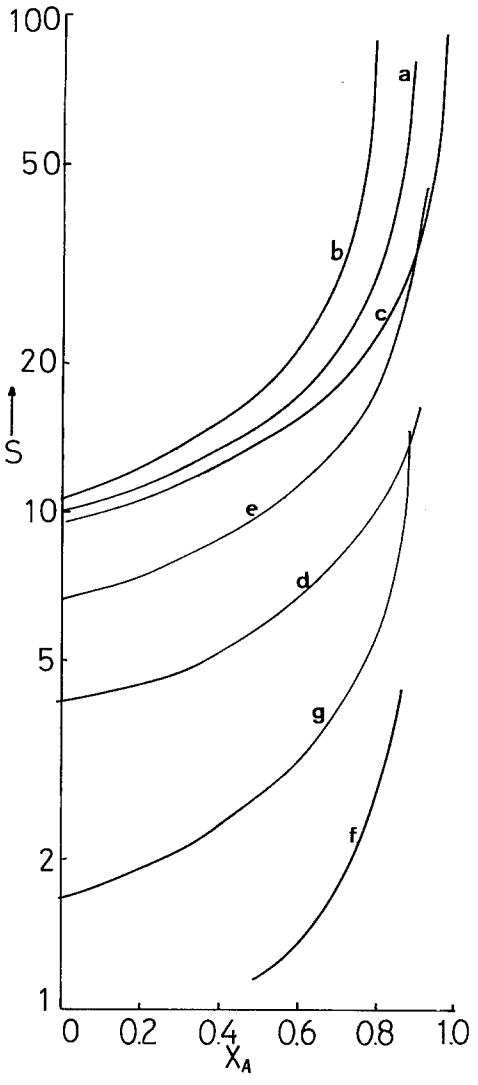

Fig. 10. Variation in selectivity with conversion for a parallel reaction of unequal Tafel slopes. $\beta_2 = \beta_1/2$; $n_1 = n_2$; $\beta_1 = 10\,V^{-1}$; $k_2 = 10^{-9}\,m\,s^{-1}$. k_2/k_1: (a–e) 1; (f) 10; (g) 5. k_1/k_L: (a) 10^{-3}; (b) 2×10^{-3}; (c) 2×10^{-4}; (d) 10^{-3}; (e) 10^{-3}; (f) 10^{-3}; (g) 10^{-3}. $i_T/(nFC_{Ao}k_1)$: (a) 100; (b) 100; (c) 100; (d) 20; (e) 50; (f) 100; (g) 100.

3.2.1. The influence of a gas evolution reaction. If this parallel reaction sequence were taking place simultaneously with, say, a hydrogen evolution reaction then the total current i_T would be

$$i_T = i_1 + i_2 + i_3$$

where i_3 is given by Equation 12.

The influence of this additional reaction on the potential time characteristics, when $n_1 = n_2$, is (following the derivation of Equation 27) given by

$$\left\{ \frac{\dfrac{\beta_2 k_{f2}}{k_{f1}^2} + \dfrac{\beta_1}{k_{f1}}}{\left(1 + \dfrac{k_{f2}}{k_{f1}}\right)^2} + \frac{n_3\beta_3 F k_{f3}\left(\dfrac{1}{k_L} + \dfrac{1}{k_{f1}} + \dfrac{k_{f2}}{k_{f1}k_L}\right)}{\left(1 + \dfrac{k_{f2}}{k_{f1}}\right)(i_T - n_3 F k_{f3})} \right\} dE = \left(\frac{S}{V}\right) dt \tag{31}$$

Following the previous assumption that $\beta_1 = \beta_2$, this can be integrated to give

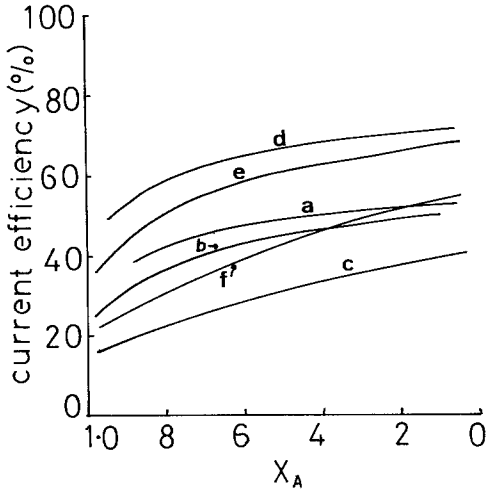

Fig. 11. Variation of overall current efficiency with conversion for a parallel reaction accompanied by solvent decomposition. $\beta_1 = \beta_2 = \beta_3$; $k_3 = 5 \times 10^{-4}\,\mathrm{mol\,m^{-2}\,s^{-1}}$, $i_T/nF = 3 \times 10^{-3}\,\mathrm{mol\,m^{-2}\,s^{-1}}$; $k_1/k_3 = 0.04$. k_2/k_1: (a) 0.5; (b) 0.5; (c) 0.5; (d) 0.1; (e) 0.1; (f) 0.1. k_{LA} ($\mathrm{m\,s^{-1}}$): (a) 10^{-3}; (b) 10^{-4}; (c) 3×10^{-5}; (d) 10^{-3}; (e) 10^{-4}; (f) 3×10^{-5}.

$$\left(1 + \frac{k_2}{k_1}\right)\left(\frac{S}{V}\right)t = \frac{1}{k_{f1o}} - \frac{1}{k_{f1}} + \left(\frac{1 + \dfrac{k_2}{k_1}}{k_L}\right) \ln\left(\frac{i_T - n_3 F k_{f30}}{i_T - n_3 F k_{f3}}\right) + n_3 F \beta_3 \int_{E_o}^{E} \left[\frac{k_{f3}}{k_{f1}\,(i_T - n_3 F k_{f3})}\right] dE \tag{32}$$

which enables the concentration–time characteristics and current efficiencies to be evaluated.

Typical variations of current efficiency with fractional conversion for this parallel reaction accompanied by solvent decomposition are presented in Fig. 11 ($\beta_1 = \beta_2 = \beta_3$). Current efficiency, as expected, decreases with conversion and is higher the smaller the ratio k_2/k_1 and the higher the mass transfer coefficient.

3.3. *A parallel–series reaction scheme*

Consider the following reaction scheme in which a dependent parallel reaction is preceded by a single reaction.

$$\mathrm{A} \xrightarrow{k_{f1}} \mathrm{B}$$

$$\mathrm{B} \xrightarrow{k_{f2}} \mathrm{C} \qquad n_1 = n_2 = n_3 = n$$

$$\mathrm{B} \xrightarrow{k_{f3}} \mathrm{D}$$

Reaction currents can be written following [7] as

$$\frac{i_1}{nF} = \frac{C_A}{Y_1} \tag{1}$$

$$\frac{i_2}{nF} = \frac{C}{Y_1 Y_3 k_{LB}} + \frac{C_B}{Y_3} \tag{33}$$

where

$$Y_3 = \frac{1}{k_{LB}}\left(1 + \frac{k_{f3}}{k_{f2}}\right) + \frac{1}{k_{f2}}$$

$$i_3 = \frac{k_{f3} i_2}{k_{f2}} \tag{34}$$

Equation 33 is derived in Appendix E.

Batch reactor design equations for this system are

$$\frac{dC_A}{dt} = -\frac{S}{V}\left(\frac{i_1}{nF}\right) \tag{4}$$

$$\frac{dC_B}{dt} = \frac{S}{VnF}(i_1 - i_2 - i_3) \tag{35}$$

$$\frac{dC_C}{dt} = \frac{S}{V}\left(\frac{i_2}{nF}\right) \tag{36}$$

$$\frac{dC_D}{dt} = \frac{S}{V}\left(\frac{i_3}{nF}\right) \tag{37}$$

During constant current operation the total current is

$$i_T = i_1 + i_2 + i_3$$

and by combining Equations 4 and 35 we obtain generally

$$C_B + 2(C_A - C_{Ao}) = -\left(\frac{Si_T}{VnF}\right)t \tag{38}$$

assuming only A present initially, at a concentration C_{Ao}. Dividing Equations 35 and 36 gives

$$\frac{dC_C}{dC_D} = \frac{k_{f2}}{k_{f3}} \tag{39}$$

If Tafel slopes for the production of C and D are equal, i.e. $\beta_2 = \beta_3$, then Equation 38 gives

$$C_C = \left(\frac{k_2}{k_3}\right)C_D \tag{40}$$

and combining with Equation 38 gives

$$C_B + 2C_C\left(1 + \frac{k_3}{k_2}\right) = \left(\frac{Si_T}{VnF}\right)t \tag{41}$$

However, to take the analysis further and obtain a solution to Equations 33 to 37 under galvanostatic operation requires numerical procedures. Under certain conditions it may be reasonable to make simplifying assumptions such as

(i) Reactions are under mass transport control and therefore rates are independent of potential which generally increases during electrolysis.
(ii) Reactions are under kinetic control with equal Tafel slopes.

The latter of these assumptions will now be considered and applied to an electro-organic synthesis from which comparisons with potentiostatic operation can be made.

If we now combine Equations 4 and 35 and substitute for reaction current densities we obtain

$$\frac{dC_B}{dC_A} = -1 + \frac{k_{f2} + k_{f3}}{k_{f1}}\left(\frac{C_B}{C_A}\right) \tag{42}$$

which integrates to

$$\frac{C_B}{C_{Ao}} = \frac{1}{1 - (k_2 + k_3)/k_1}\left[\left(\frac{C_A}{C_{Ao}}\right)^{(k_2 + k_3)/k_1} - \frac{C_A}{C_{Ao}}\right] \tag{43}$$

when $k_2 + k_3 \neq k_1$, or

$$\frac{C_B}{C_{Ao}} = -\left(\frac{C_A}{C_{Ao}}\right) \ln\left(\frac{C_A}{C_{Ao}}\right) \tag{44}$$

when $k_2 + k_3 = k_1$. Combining Equations 38 and 43 we can obtain both C_A and C_B as a function of time and with Equation 40, the complete spectrum of products.

One of the features of this type of reaction sequence is that the intermediate B goes through a maximum concentration, C_{Bmax}, given by

$$\frac{C_{Bmax}}{C_{Ao}} = \left(\frac{k_1}{k_2 + k_3}\right)^{k_2 + k_3/k_2 + k_3 - k_1} \tag{45}$$

when $k_2 + k_3 \neq k_1$, or

$$\frac{C_{Bmax}}{C_{Ao}} = \frac{1}{\exp(1)} \tag{46}$$

when $k_2 + k_3 = k_1$ and at reaction times given by

$$\frac{i_T S}{nFVC_{Ao}}(t_{max}) = 2 - \frac{C_{Bmax}}{C_{Ao}}\left[1 + \frac{2(k_2 + k_3)}{k_1}\right] \tag{47}$$

If B is the desired product and C and D are of no real value then this fixes the maximum electrolysis time for this reaction. The greater the value of the ratio k_1/k_2 the greater the conversion to intermediate B and the later it occurs on the conversion or time scale.

3.3.1. Potential variation. Potential variation during galvanostatic operation is an important factor of operation not only because of energy considerations (which will generally be higher than in potentiostatic operation) but may give some insight into the applicability of the model by way of assessing conditions for solvent decomposition. This variation in potential is given for this model as

$$\exp[\beta(E - E_o)] = \left[1 - \frac{Si_T t}{2nFVC_{Ao}} + \frac{C_B}{C_{Ao}}\left(\frac{k_2 + k_3}{k_1}\right) - 1/2\right]^{-1} \tag{48}$$

and up to a time for maximum production of B as

$$\exp[\beta(E - E_o] = 1/2\left(\frac{k_2 + k_3}{k_1}\right)^{(k_2 + k_3 - k_1)/k_1} \tag{49}$$

when $k_2 + k_3 \neq k_1$, or

$$\beta(E - E_o) = 1 - \ln(2)$$

when $k_2 + k_3 = k_1$.

3.3.2. Process example: the production of glyoxylic acid. In the electrolytic production of glyoxylic acid from aqueous oxalic acid solutions it was found that the major loss of efficiency (other than through organic byproducts) is due to hydrogen evolution resulting from cathode contamination. This means that the reactor performance in terms of the concentration–time characteristics cannot be predicted by the proposed analysis, and what is required is some representation of electrode deactivation. This experimental finding and an analysis of electrode deactivation is the subject of a following paper [10].

A feature of interest in this reaction system is the parallel reaction step involving the further reduction of glyoxylic acid to glycolic acid (C) and glyoxal (D). Experimental data for the production of these two byproducts are presented in Fig. 12, in terms of their ratio of concentration,

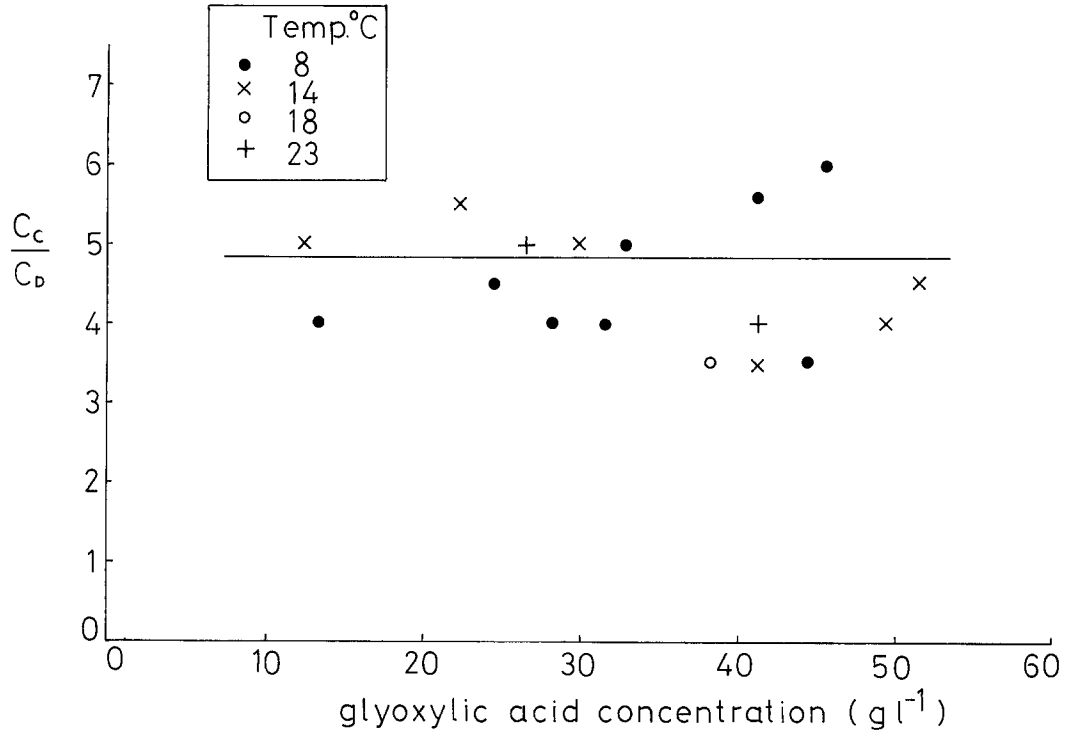

Fig. 12. Variation of the ratio of glycolic acid and glyoxal byproducts with the production level of glyoxylic acid. Lead cathode, temperatures 8–18° C, current densities 500–2500 A m^{-2}.

C_C/C_D versus the production level of glyoxylic acid. The experimental operating conditions relevant to these data are given in [11] and [13]. Electrolysis cells and operations were as described in Section 2. It is apparent from Fig. 12 that a precise analysis of the mechanism of the parallel reaction step is not feasible because of the wide spread in ratios of approximately 3.5 to 6. At best, a value of the ratio of rate constants k_2/k_3 of approximately 5 can be suggested and because of the apparently invariable nature of the concentration ratio with respect to glyoxylic acid concentration (hence duration of electrolysis), an assumption of equal Tafel slopes, i.e. $\beta_2 = \beta_3$ can be applied.

Continuing now with the process example in which the following kinetic data, taken from [11] and [12], are representative of the production of glyoxylic acid by the electroreduction of oxalic acid solutions acidified with sulphuric acid: $k_1/k_2 = 2.65$ with $k_2/k_3 = 5$. Tafel slopes for the electroreduction of oxalic acid (A) and glyoxylic acid (B) are both approximately 120 mV^{-1}.

The data in Fig. 13 are plotted as a function of two dimensionless time parameters τ_g and τ_p for galvanostatic and potentiostatic operation respectively. These data are valid for any value of current density or electrode potential under their respective modes of operation. The maximum concentration of product glyoxylic acid under either operating mode is identical. The advantage of galvanostatic operation is in the shorter reaction times to produce glyoxylic acid, but the consequence of this is a greater production of byproduct and lower efficiency.

In this and a large number of similar systems it is likely that two major factors will detract from this ideal performance:

(i) Limitations in mass transport which will become more important at higher potentials. In this case the maximum possible conversion to intermediate B will be reduced.

(ii) Decomposition of solvent which is likely to be more significant at higher potentials and more pronounced during galvanostatic operation.

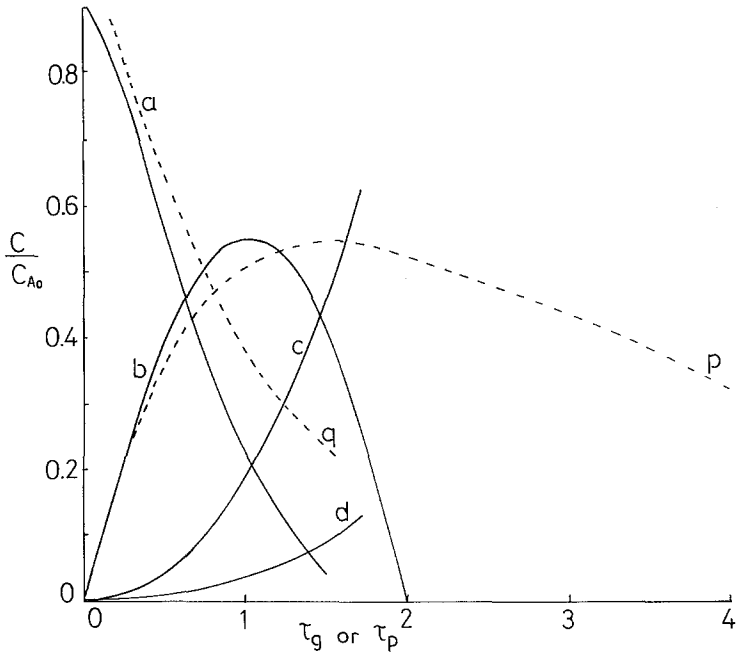

Fig. 13. Predicted performance of the electroreduction of oxalic acid during galvanostatic operation showing typical concentration time profiles. Galvanostatic operation (——): (a) oxalic acid; (b) glyoxylic acid; (c) glycolic acid; (d) glyoxal. Potentiostatic operation (– – –): (p) glyoxylic acid; (q) oxalic acid. $\tau_g = (Si_T t)/(VnFC_{Ao})$. $\tau_p = (k_{f1} St)/V$.

4. Conclusions

The application of reaction engineering techniques to parallel electrochemical reactions during constant current operation has been broadly demonstrated for the case of batch reactions. For flow electrolyses operating continuously, the problem should prove no more difficult as we need only consider space time as opposed to real time. With recycle operation the models can be readily extended to include inlet concentration of all product species from the recycle stream.

It has been shown that by applying suitable approximations to the kinetics of these parallel reaction schemes, useful analytical equations representing reactor behaviour can be derived. The main approximation in integer ratios of Tafel slopes frequently occurs in practical situations and allows quite complex reaction networks to be analysed using standard techniques. These techniques may be extended to reactions involving two or more components, especially if in each step of the reaction scheme the second reactant is common.

Appendix A

Derivation of Equation 14

For galvanostatic operation of a reaction obeying Tafel kinetics in the presence of solvent decomposition (eg. hydrogen evolution) the total current density is given by Equation 13 which on differentiation gives

$$0 = \frac{n_1 F}{Y_1}\left(\frac{dC_A}{dt}\right) + \frac{n_1 F C_A}{k_{f1}}\left(\frac{dE}{dt}\right)\left(\frac{\beta_1}{Y_1^2}\right) + n_3 F \beta_3 k_{f3}\left(\frac{dE}{dt}\right) \tag{A1}$$

The batch reactor design equation for component A can be written as

$$\frac{dC_A}{dt} = -\frac{S}{Vn_1 F}(i_T - n_3 F k_{f3}) \tag{A2}$$

Eliminating dC_A/dt between Equations A1 and A2 gives

$$\frac{S(i_T - n_3 F k_{f3})}{VY_1} = \left(\frac{n_1 F C_A \beta_1}{k_{f1} Y_1^2} + n_3 F \beta_3 k_{f3}\right)\left(\frac{dE}{dt}\right) \tag{A3}$$

Substituting now for C_A using Equation 13 gives

$$\left(\frac{\beta_1}{k_{f1}} + \frac{n_3 F \beta_3 k_{f3} Y_1}{i_T - n_3 F k_{f3}}\right)\frac{dE}{dt} = \left(\frac{S}{V}\right)t \tag{A4}$$

With the initial electrode potential given by E_o, this integrates to give Equation 14.

Appendix B

Derivation of Equation 22

For two independent reactions occurring simultaneously with oxygen evolution, all under kinetic control, the total current density is given by

$$\frac{i_T}{F} = \exp^{\beta E}(n_1 k_1 C_A + n_2 k_2 C_C + n_3 k_3) \tag{B1}$$

Substitution in the batch reactor design Equation 4 for species A gives

$$-\frac{dC_A}{dt} = \frac{S i_T k_1}{VF}\left(\frac{C_A}{n_1 k_1 C_A + n_2 k_2 C_C + n_3 k_3}\right) \tag{B2}$$

Separating variables and substituting Equation 10 for C_C gives

$$\left[n_1 k_1 + \frac{n_3 k_3}{C_A} + n_2 k_2 \frac{C_{Co}}{C_A}\left(\frac{C_A}{C_{Ao}}\right)^{k_2/k_1}\right]dC_A = -\frac{S k_1 i_T dt}{VF} \tag{B3}$$

Integrating this equation gives Equation 22.

Appendix C

Derivation of Equation 27

For the dependent parallel reaction scheme described in Section 3.2, Equations 23 and 25 can be combined to eliminate the surface concentration C_A^S to give the reaction current density for step A → B as

$$\frac{i_1}{n_1 F} = \frac{C_A}{\frac{1}{k_L} + \frac{1}{k_{f1}} + \frac{k_{f2}}{k_{f1} k_L}} \tag{C1}$$

For galvanostatic operation with $i_1 + i_2 = i_T$ the above equation can be combined with Equation 24 to give the concentration C_A as

$$C_A = \frac{\frac{i_T}{n_1 F}\left(\frac{1}{k_L} + \frac{1}{k_{f1}} + \frac{k_{f2}}{k_{f1} k_L}\right)}{1 + \frac{n_2 k_{f2}}{n_1 k_{f1}}} \tag{C2}$$

which can be differentiated to give

$$\frac{dC_A}{dt} = \frac{i_T}{n_1 F}\left\{\frac{\left(\frac{1}{k_L}+\frac{1}{k_{f1}}+\frac{k_{f2}}{k_{f1}k_L}\right)\left[\frac{n_2}{n_1}(\beta_1-\beta_2)\frac{k_{f2}}{k_{f1}}\right]}{\left(1+\frac{n_2 k_{f2}}{n_1 k_{f1}}\right)^2}+\frac{\frac{(\beta_2-\beta_1)k_{f2}}{k_L k_{f1}}-\frac{\beta_1}{k_{f1}}}{1+\frac{n_2 k_{f2}}{n_1 k_{f1}}}\right\}\frac{dE}{dt} \tag{C3}$$

The batch reactor design Equation 26 can be written in terms of total current density as

$$\frac{dC_A}{dt} = -\frac{S}{V}\left[\frac{1+k_{f2}/k_{f1}}{1+\frac{n_2 k_{f2}}{n_1 k_{f1}}}\left(\frac{i_T}{n_1 F}\right)\right] \tag{C4}$$

Combining this with Equation C3 for dC_A/dt gives Equation 27, describing the variation of electrode potential with time.

Appendix D

Integration of Equation 27 ($n_1 = n_2$)

Substituting $u = \exp[(\beta_2 - \beta_1)E]$, we obtain

$$-\left(\frac{S}{V}\right)dt = -\frac{\beta_2 k_2}{(\beta_2-\beta_1)k_1^2}\left[\int\frac{u^{-\beta_1/(\beta_2-\beta_1)}}{\left(1+\frac{k_2 u}{k_1}\right)^2}\right]du - \frac{\beta_1}{(\beta_2-\beta_1)k_1}\left[\int\frac{u^{-\beta_2/(\beta_2-\beta_1)}}{\left(1+\frac{k_2 u}{k_1}\right)^2}\right]du \tag{D1}$$

When $\beta_2 = \beta_1/2$ this becomes

$$-\left(\frac{S}{V}\right)dt = \frac{k_1}{k_2^2}\left[\int\frac{u^2}{\left(1+\frac{k_2 u}{k_1}\right)^2}\right]du + \frac{2}{k_1}\int\frac{u\,du}{\left(1+\frac{k_2 u}{k_1}\right)^2} \tag{D2}$$

and on integration we obtain

$$-\left(\frac{S}{V}\right)t = \frac{k_1}{k_2^2}\left[1+\frac{k_2 u}{k_1}-2\log\left(1+\frac{k_2 u}{k_1}\right)-\frac{1}{1+(k_2 u/k_1)}\right]_{u(t=0)}^{u(t=t)} + \frac{2k_1}{k_2^2}\left[\log\left(1+\frac{k_2 u}{k_1}\right)+\frac{1}{\left(1+\frac{k_2 u}{k_1}\right)}\right]_{u(t=o)}^{u(t=t)} \tag{D3}$$

which simplifies to

$$-\left(\frac{S}{V}\right)t = \frac{k_1}{k_2^2}\left[1+\frac{k_2 u}{k_1}+\frac{1}{\left(1+\frac{k_2 u}{k_1}\right)}\right]_{u(t=o)}^{u(t=t)} \tag{D4}$$

Appendix E

Derivation of Equation 33

For the reaction scheme in Section 3.3, current densities for the three steps can be written as

$$\frac{i_1}{nF} = k_{f1} C_A^S \tag{E1}$$

$$\frac{i_1}{nF} = k_{LA}(C_A - C_A^S) \tag{E2}$$

$$\frac{i_2}{nF} = k_{f2} C_B^S \tag{E3}$$

$$\frac{i_3}{nF} = k_{f3} C_B^S \tag{E4}$$

$$\frac{(i_1 - i_2 - i_3)}{nF} = k_{LB}(C_B^S - C_B) \tag{E5}$$

Combining Equations E1 and E2 to eliminate C_A^S gives Equation 1. Combining Equations E3, E4 and E5 to eliminate C_B^S and i_3 gives

$$\frac{i_1 - i_2\left(1 + \frac{k_{f3}}{k_{f2}}\right)}{nF} = k_{LB}\left(\frac{i_2}{nFk_{f2}} - C_B\right) \tag{E6}$$

which rearranges to give

$$\frac{i_2}{nF}\left[\frac{1}{k_{f2}} + \frac{1}{k_{LB}}\left(1 + \frac{k_{f3}}{k_{f2}}\right)\right] = \frac{i_1}{nFk_{LB}} + C_B \tag{E7}$$

Substituting for i_1 using Equation 1 and rearranging leads to Equation 33 which gives the reaction current density, i_2.

References

[1] M. Fleischmann and R. E. W. Jansson, *J. Appl. Electrochem.* **9** (1979) 427.
[2] O. Levenspiel 'Chemical Reaction Engineering' 2nd Ed, J. Wiley, New York (1972).
[3] F. Goodridge and A. R. Wright in 'Comprehensive Treatise of Electrochemistry' Vol. 6 (edited by E. Yeager, J. O. M. Bockris, B. E. Conway and S. Sarangapani) Plenum Press, New York (1983).
[4] G. P. Sakellaropoulos and G. A. Francis, *J. Electrochem. Soc.* **126** (1979) 1928.
[5] G. P. Sakellaropoulos, *AIChEJ* **25** (1979) 781.
[6] G. P. Sakellaropoulos and G. A. Francis, *J. Chem. Tech. Biotechnol.* **30** (1980) 102.
[7] K. Scott, *Electrochim. Acta* **30** (1985) 235.
[8] *Idem, ibid.* **30** (1985) 245.
[9] V. Krishnan, K. Ragupathy and H. V. K. Udupa, *J. Appl. Electrochem.* **8** (1978) 169.
[10] K. Scott, submitted to *Chem. Eng. Res. Design.*
[11] K. Scott, PhD Thesis University of Newcatle-upon-Tyne, UK (1977).
[12] D. J. Pickett and K. S. Yap, *J. Appl. Electrochem.* **4** (1974) 17.
[13] F. Goodridge, K. Lister, R. E. Plimley and K. Scott, *J. Appl. Electrochem.* **10** (1980) 55.